Zn^{2+} fluorescent chemosensors and the influence of their spacer length on tuning Zn^{2+} selectivity †

Tae Woo Kim, Jung-hyun Park and Jong-In Hong *

School of Chemistry and Molecular Engineering, Seoul National University, Seoul 151-747, Korea. E-mail: jihong@plaza.snu.ac.kr

Received (in Cambridge, UK) 14th January 2002, Accepted 28th February 2002
First published as an Advance Article on the web 5th April 2002

Zn^{2+} fluorescent chemosensors based on the chelation-enhanced fluorescence (CHEF) mechanism were prepared and fine-tuning of their Zn^{2+} selectivity was achieved by control of the spacer length. The fluorescence emission response to metal ions shows a fluorescence decrease for Co^{2+}, Cu^{2+} and Ni^{2+} and an increase for Ca^{2+}, Cd^{2+} and Zn^{2+}. Maximum Zn^{2+} selectivity over Ca^{2+} and Cd^{2+} was achieved with **3**. The basic binding properties (stoichiometry, apparent dissociation constant, and pH dependence) were measured by fluorescence spectroscopy. Analysis of the Job plot for the **3**–Zn^{2+} complex indicates the formation of a 1 :1 complex. The apparent dissociation constant K_d was determined as 0.98 (±0.43) nM for **3**–Zn^{2+} at pH 7.5 [50 mM HEPES buffer $I = 0.1$ ($NaNO_3$)]. The plateaus in the fluorescence intensity of **2** and the **2**–Zn^{2+} complex in regions with a pH exceeding 7 imply that the fluorescence measurements should be little affected by physiological pH changes.

Introduction

Zinc is an important divalent cation in biological systems, influencing DNA synthesis, microtubule polymerization, gene expression, apoptosis, immune system function and the activity of enzymes such as carbonic anhydrase and matrix metalloproteinases (MMP).[1] Quantitative analysis of trace Zn^{2+} ions with a selective analytical ligand has become extremely important for environmental and biological applications. Owing to the high sensitivity and selectivity of such sensors, many groups have investigated fluorescent chemosensors for Zn^{2+}.[2]

The most widely applied probes for cellular zinc are arenesulfonamides of 8-aminoquinoline such as TSQ[3] and Zinquin.[2e,f,4] Other types of zinc indicator are also commercially available in cell-permeable or cell-impermeable form: FuraZin™, IndoZin™, FluoZin™, Newport Green™, *etc*.[5]

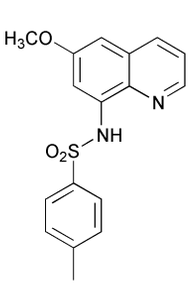

TSQ

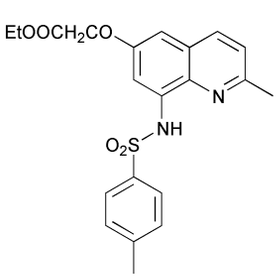

Zinquin Ester

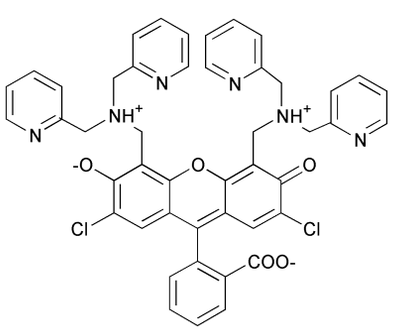

Zinpyr-1

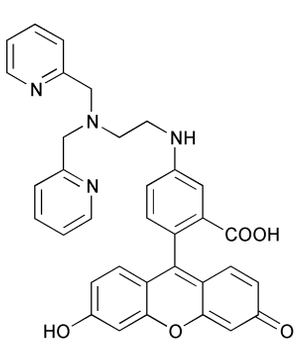

ZnAF-1

Recently, cell-permeable Zn^{2+} sensor molecules based on fluorescein (Zincpyr-1,[2b] ZnAF[6]) were reported and their biological applications were investigated in a cellular system.

The main problem of Zn^{2+} fluorescent sensing is low selectivity between Zn^{2+} and Cd^{2+}. Dansylamidoethyl-pendant‡ cyclen[2a] and Zincpyr-1,[2b] reported respectively by Kimura and Tsien, do not show Zn^{2+}/Cd^{2+} selectivity. As to their relative fluorescence intensity (F/F_0), they slightly prefer to bind with Cd^{2+} rather than with Zn^{2+}: F/F_0 = 4.9 (Zn^{2+}), 5.1 (Cd^{2+}) for dansylamidoethyl-pendant cyclen and 2.8 (Zn^{2+}), 3.4 (Cd^{2+}) for Zincpyr-1. Nagano and co-workers developed the first Zn^{2+} sensor molecule (ZnAF-1) that can distinguish Cd^{2+} from Zn^{2+}.[6] The selectivity is due to the switching carboxylate/nitrogen coordination caused by the different ionic radii. Clarification of other factors controlling Zn^{2+}/Cd^{2+} selectivity is still required.

The development of fluorescent microscopy techniques and the increasing need for bioanalytical tools has given rise to fluorescent probes that can monitor a specific analyte in real

† Electronic supplementary information (ESI) available: job plot, partial ^{1}H NMR spectra of free **3** and the **3**–Zn^{2+} complex, Ca^{2+} and Mg^{2+} interference for Zn^{2+} sensing of **3**, K_d measurements, and buffer preparation. See http://www.rsc.org/suppdata/p2/b2/b200462c/
‡ The IUPAC name for dansyl is 5-dimethylaminonaphthylsulfonyl.

time. The trend will demand new criteria to complement the shortcomings of the traditional fluorescent sensor, namely working in the physiological environment, overcoming autofluorescence, cell permeability, *etc*. Therefore, the novel design of fluorescent sensors suitable for biological applications is a challenging task.[7]

Results and discussion

Design and synthesis of the fluorescent chemosensors, 2, 3, 4 and 6

For a fluorescent metal ion chemosensor with biological application (*e.g.*, cell-permeable Zn^{2+} sensor), the sensor can be disassembled into three components as shown in Fig. 1: binder,

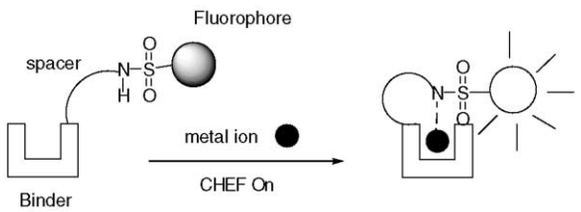

Fig. 1 Design of a fluorescent chemosensor using the chelation-enhanced fluorescence of dansyl sulfonamide.

fluorophore, and spacer. We thought that the Zn^{2+} selectivity would be controlled by the spacer length between the binder and fluorophore.

A binder needs to fulfil the following requirements: sub-nM K_d in aqueous media and neutral working pH. In order to operate a sensor in on/off mode, a well-known fluorescent enhancement mechanism is essential. Since the effect of spacer length on the metal ion selectivity is of great interest, the spacer needs to be readily modifiable. We incorporated the bis(2-pyridylmethyl)amine (di-2-picolylamine or DPA) moiety into our probe for chelating zinc. The Zn^{2+}–DPA complex has a stability constant log K (1 : 1 complex) of 7.6 at 25 °C, I = 0.1.[8] We selected a dansyl moiety as the reporting group,[9] in which sulfonamide has been applied to the chelation-enhanced fluorescence (CHEF) system.[2a,e,f,10] In our work, the DPA and dansyl units were connected by a suitable spacer, $–(CH_2)_n–$ (n = 2, 3, 4, 6). The fluorescent probes, **2**, **3**, **4**, and **6** were prepared as shown in Fig. 2. In the cases of n = 4 or 6, reaction of $Br(CH_2)_nNHDs$ and DPA resulted in an intramolecular cyclization without DPA addition.

Fluorescence emission response to metal ions

At pH 7.5 {50 mM HEPES [*N*-(2-hydroxyethyl)piperazine-*N*′-(ethane-2-sulfonic acid)] buffer, I = 0.1 ($NaNO_3$)}, the fluorescence emission responses of **2**, **3**, **4**, **6** with 1 equiv. metal ions are shown in Fig. 3. The trend of fluorescence quenching and enhancement basically agrees with that described in Kimura's report:[2a] the fluorescence decreases for Co^{2+}, Cu^{2+} and Ni^{2+}, and increases for Ca^{2+}, Cd^{2+}, and Zn^{2+}. However, the metal selectivity itself is sensitive to the spacer length. Maximum Zn^{2+} selectivity against Ca^{2+} and Cd^{2+} was achieved with **3** (Table 1).

Since Cd^{2+} is not present to a significant extent in the cellular environment, the major competitors of Zn^{2+} are biological metal cations such as Na^+, K^+, Ca^{2+} and Mg^{2+}.[2a] The Zn^{2+}-dependent fluorescence is unaffected by the presence of mM concentrations of Na^+ [buffer ionic strength, I = 0.1 ($NaNO_3$)]. The competition experiments between Zn^{2+} and Ca^{2+}/Mg^{2+} reveal that 100 equivalents of Ca^{2+}/Mg^{2+} have no influence on Zn^{2+} fluorescence. The Zn^{2+} selectivity over alkali or alkaline earth cations will come from the inherent binding properties of bis(2-pyridylmethyl)amine. In addition, the metal selectivity seems to be related to the extra binding of the pendant sulfonamide N^- to zinc at the fourth coordination site in the **3**–Zn^{2+} complex. Subtle factors, such as spacer length or alkyl chain conformation in the complex, should influence the Zn^{2+} selectivity under physiological pH.

Table 1 Properties of the complexes of probe ***n*** with Ca^{2+}, Cd^{2+} and Zn^{2+}, respectively[a]

Probes	Zn^{2+} [b]	Ca^{2+} [b]	Cd^{2+} [b]	$SF_{Zn/Ca}$ [c]	$SF_{Zn/Cd}$ [c]
2	4.03	4.62	4.89	0.87	0.82
3	3.72	0.33	1.36	*11.3*	*2.74*
4	0.97	1.51	1.36	0.64	0.71
6	1.21	0.83	1.00	1.46	1.21

[a] Data were acquired with excitation at 330 nm in 50 mM HEPES, pH 7.5, I = 0.1 ($NaNO_3$), [***n***] = 5 μM, and $[M^{2+}]$ = 5 μM. [b] Fluorescence intensity of the complexes at $\lambda_{max}(Zn^{2+})$ was normalized such that the fluorescence intensity at λ_{max}(free) = 1. λ_{max}(free) and $\lambda_{max}(Zn^{2+})$, respectively, mean the wavelength of maximum emission for the probe in the absence of metal ion and for the probe–Zn^{2+} complex. [c] The selectivity factor (SF) is defined as the fluorescence intensity ratio of Zn^{2+}/Ca^{2+} or Zn^{2+}/Cd^{2+}. Values of SF of greater than 1 indicate Zn^{2+} selectivity; value of less than 1 indicate Ca^{2+} or Cd^{2+} selectivity.

Binding stoichiometry

In order to investigate the possibility of biological application, the binding stoichiometry, K_d, and pH dependence of **3** were examined. Analysis of the Job plot[11] for the **3**–Zn^{2+} complex (molar fraction 0.45 at the maximum increase in fluorescence) and the value of 100% for the abundance of the $[\mathbf{3}–Zn^{2+}]^+$ peak (m/z = 552 for $C_{27}H_{30}N_5O_2SZn$, calcd. 552.14) in FAB-MS indicate the formation of a 1 : 1 complex. Two doublets (3.90, 4.13 ppm, J = 16 Hz) in the equimolar **3**–Zn^{2+} complex imply that the **3**–Zn^{2+} complex adopts a restricted conformation and loses the symmetry plane of free **3**. This pattern results from the coordination of the sulfonamide N^- anion to zinc at the fourth ligand site.

Dissociation constant, K_d

To minimize the experimental error due to the large binding constant, the apparent dissociation constant K_d was measured by competition with the known nitrilotriacetic acid (NTA) ligand. In our NTA/**3** competition study, we assumed that each of the formation constants for Zn^{2+} should be sufficiently similar[8] and the concentration difference between $[NTA]_{total}$ (1 mM) and $[\mathbf{3}]_{total}$ (5 μM) is large enough. In terms of results, the value of $[Zn^{2+}]_{free}$ calculated from a system containing only NTA is still valid in system with NTA/**3** competition.

The apparent dissociation constant (K_d) was determined as 0.98 (± 0.43) nM for **3**–Zn^{2+} (Fig. 4). Ligand **2** also has a similar K_d, 0.19 (± 0.54) nM. These values indicate that **2** and **3** can be used in the sub-nM range, which affords sufficient sensitivity for cellular Zn^{2+} detection. A blue shift of the fluorescence of **3** (λ_{max} = 540 nm) occurred upon **3**–Zn^{2+} complexation (λ_{max} = 522 nm). Similar fluorescence blue shifts and fluorescence intensity enhancements were reported for dansylamide complexation with carbonic anhydrase.[2a,12] The large blue shift for **3**–Zn^{2+} can be accounted for by the deprotonation of dansylamide at neutral pH. Despite a small enhancement in fluorescence intensity, free **3** shows a blue shift in high pH regions.

From the experimental concentration (~5 μM) and large log K_f(ZnL) (7.57) and log K_f(CdL) (6.44) values of L (DPA),[8] we can assume that equimolar metal cation is present in an almost complexed state and so the peculiar fluorescence responses cannot be explained in terms of the difference in K_d. At present, we cannot give an adequate explanation for the selectivity of **3** for Zn^{2+} over Cd^{2+}. However, we think that the different radii and electronic configuration of Zn^{2+} and Cd^{2+} might play an important role in the fluorescence response of dansylamide coordination.

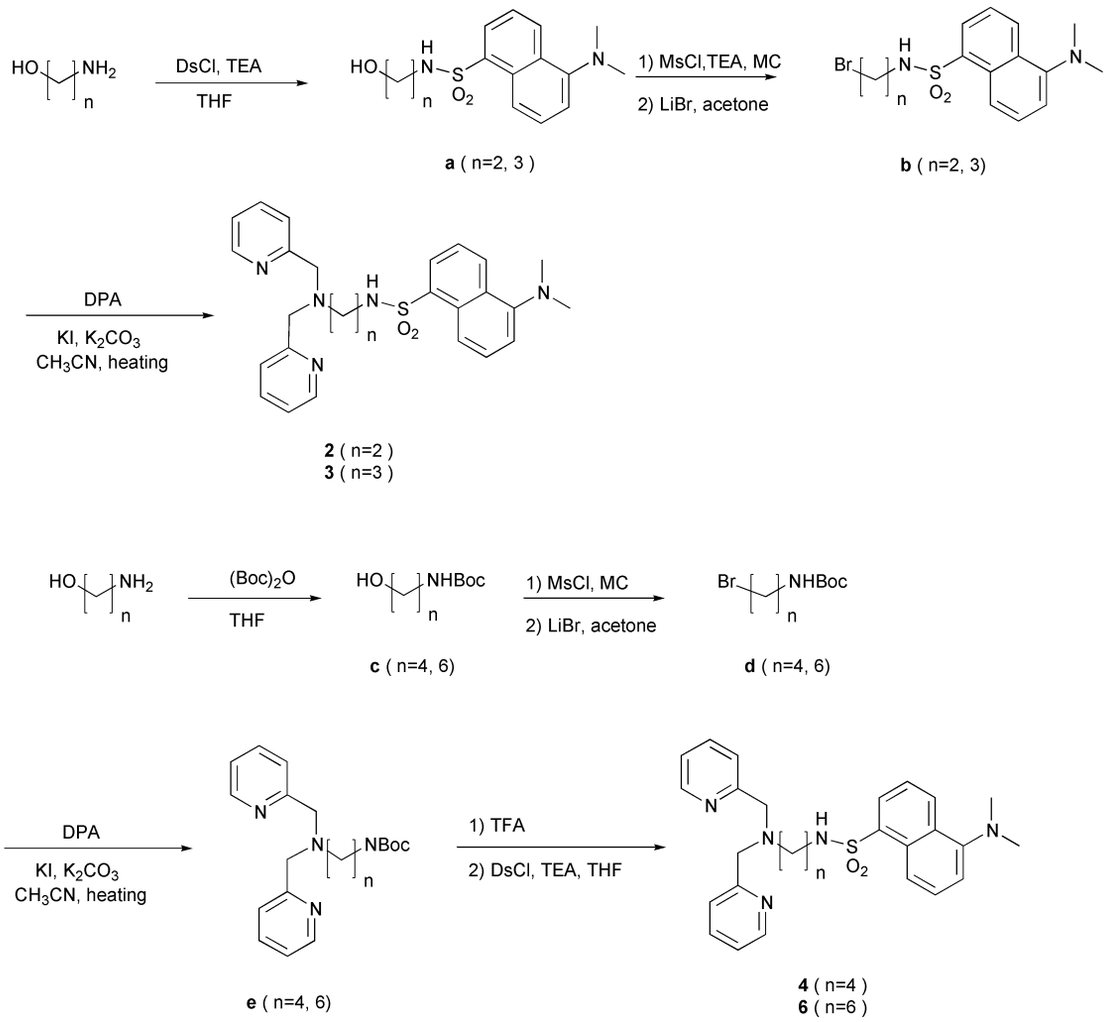

Fig. 2 *Reagents*: DsCl = dansyl chloride, MsCl = methanesulfonyl chloride, MC = methylene chloride.

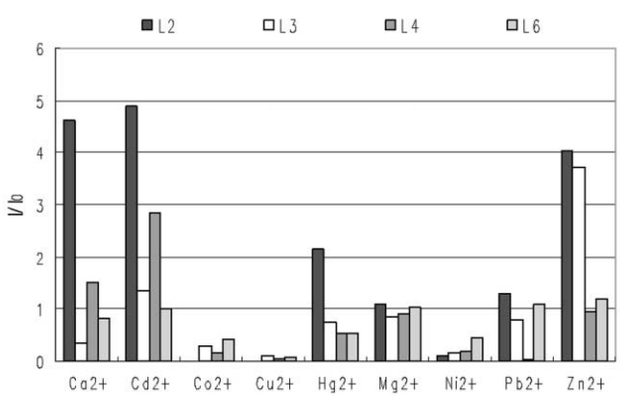

Fig. 3 Fluorescence emission response profiles of **2**, **3**, **4** and **6** (see the footnotes of Table 1 for experimental details).

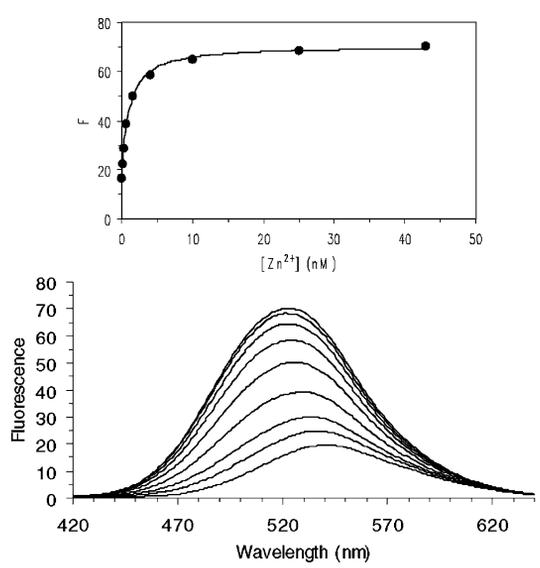

Fig. 4 Fluorescence emission response of **3** to buffered Zn^{2+} solutions. The first 10 spectra shown correspond to the free Zn^{2+} concentrations between 0 and 43 nM. Box: the observed data (●) were analyzed by nonlinear least-squares fitting (solid line).

pH Dependence

Intracellular pH changes are observed in many cells exposed to certain biological stimuli. It is well known that intracellular acidification occurs during apoptosis following cytotoxic insult.[13] Thus, the fluorescence of probes can be changed by intracellular pH changes under physiological conditions. In order to check the working pH, the effect of pH on the fluorescence emission was measured (Fig. 5).

The fluorescence intensity of solutions of 5 μM **2** (or **3**) and 5 μM **2** (or **3**) + 5 μM $Zn(ClO_4)_2$ in appropriate buffers was measured at each λ^{em}_{max} (330 nm excitation). The fluorescence intensity of **2** and the **2**–Zn^{2+} complex displays plateaus in regions with a pH above 7. Thus, the fluorescence measurements should be little affected by physiological pH changes. However, **3** and the **3**–Zn^{2+} complex show some fluctuations in fluorescence intensity in the region above pH 7 and so the Zn^{2+} measurement for probe **3** contains an error of ~10%.

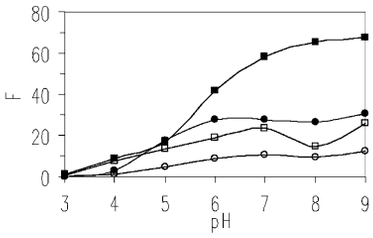

Fig. 5 Effect of pH on the fluorescence intensity (**2** ○, **2**–Zn^{2+} complex ●, **3** □, **3**–Zn^{2+} complex ■) at each λ_{max}, 5 μM.

Conclusion

We have designed Zn^{2+} fluorescent chemosensors based on the CHEF mechanism and prepared Zn^{2+} fluorescent chemosensors, bis(2-pyridylmethyl)amine-dansyl conjugates with different spacer length (n = 2, 3, 4, 6). Their metal selectivity and basic binding properties (stoichiometry, K_d, and pH dependence) were measured by fluorescence spectroscopy. Their fluorescence emission responses to metal ions show a fluorescence decrease for Co^{2+}, Cu^{2+} and Ni^{2+}, and an increase for Ca^{2+}, Cd^{2+} and Zn^{2+} The maximum selectivity for Zn^{2+} over Ca^{2+} and Cd^{2+} was achieved with probe **3**. It seems that the metal selectivity is related to the extra binding of the pendent sulfonamide N^- anion to zinc at the fourth coordination site in the **3**–Zn^{2+} complex. Analysis of the Job plot for the **3**–Zn^{2+} complex indicates the formation of a 1 : 1 complex. The apparent dissociation constant K_d was determined as 0.98 (± 0.43) nM for **3**–Zn^{2+} at pH 7.5 [50 mM HEPES buffer I = 0.1 ($NaNO_3$)]. The plateaus in the regions with pH above 7 imply that the fluorescence measurements should be little affected by physiological pH changes.

Experimental

Fluorescence (JASCO FP 750) spectrometers were used. The slit width was 5 nm for both excitation and emission. Probes were dissolved in DMSO to obtain 10 mM stock solutions. Samples were prepared by dilution of the stock solution with 50 mM HEPES buffer, I = 0.1 ($NaNO_3$).

Compounds 2 and 3

To a solution of 2-aminoethanol (23 mg, 0.37 mmol) in THF were added TEA (60 μL) and DsCl (100 mg, 0.37 mmol). After stirring for 1 h at rt, all the volatile components were evaporated and the residue was partitioned between ethyl acetate and water. The organic phase was washed with water (×3), then dried with Na_2SO_4. Flash chromatographic purification (hexane–ethyl acetate = 1 : 2) afforded **a** (n = 2) (91 mg, 0.33 mmol, 89% yield).

To a solution of **a** (n = 2) in MC were added TEA (50 μL) and MsCl (32 μL, 0.40 mmol). After stirring for 1 h at rt, 20 mL of additional acetone and 10 equiv. of LiBr (343 mg, 4.00 mmol) were added. After overnight stirring, all the volatile components were evaporated and the residue was partitioned between ethyl acetate and water. The organic phase was washed with water (×3), then dried in Na_2SO_4. Flash chromatographic purification (hexane–ethyl acetate = 1 : 2) afforded **c** (n = 2) (92 mg, 82% yield).

To a solution of **c** (n = 2) in acetonitrile were added 2 equiv. of KI (89.3 mg), 2 equiv. of K_2CO_3 (74 mg), and 2 equiv. of DPA (107 mg). After the reaction mixture had been moderately heated and refluxed for over 12 h, all the volatile components were evaporated and the residue was partitioned between ethyl acetate and water. The organic phase was washed with water (×3), then dried in Na_2SO_4. Flash chromatographic purification (MC–methanol = 20 : 1) afforded **2** (99 mg, 78% yield).

The same procedure was applied to the synthesis of **3**.

Compound **2**: ^{1}H NMR (300 MHz, $CDCl_3$, 25 °C): δ 2.78 (t, J 5.9 Hz, 2H, N$CH_2$$CH_2$), 2.87 (s, 6H, N($CH_3$)$_2$), 3.04 (br, 2H, CH_2CH_2NH), 3.76 (s, 4H, PyCH_2N), 7.11–7.18 (m, 5H), 7.43–7.52 (m, 4H), 8.24 (br, 1H, NHSO$_2$), 8.49 (d, J 3.0 Hz, 1H), 8.60 (d, J 4.2 Hz, 2H); ^{13}C NMR (75 MHz, $CDCl_3$, 25 °C): δ 41.4, 45.4, 53.1, 59.5, 114.9, 119.6, 122.2, 123.0, 123.2, 125.9, 127.7, 129.2, 129.8, 135.4, 136.7, 148.9, 151.7, 158.5; FAB-MS (MNBA): m/z = 476 (31%, obsd), 476.21 (calcd for [M + H]$^+$).

Compound **3**: ^{1}H NMR (300 MHz, $CDCl_3$, 25 °C): δ 1.67 (br, 2H, $CH_2CH_2CH_2$), 2.58 (t, 2H, J 5.9 Hz, 2H, N$CH_2$$CH_2$), 2.89 (s, 6H, N($CH_3$)$_2$), 3.03 (br, 2H, CH_2CH_2NH), 3.69 (s, 4H, PyCH_2N), 7.11–7.30 (m, 5H), 7.40–7.50 (m, 3H), 8.29 (d, J 7.3 Hz, 2H), 8.51 (d, J 8.5 Hz, 1H), 8.58 (d, J 8.6 Hz, 1H), 8.70 (d, J 4.8 Hz, 2H), 9.04 (br, 1H, NHSO$_2$); ^{13}C NMR (75 MHz, $CDCl_3$, 25 °C): δ 26.4, 41.9, 45.8, 52.1, 59.8, 115.3, 120.2, 122.6, 123.3, 123.7, 126.3, 127.9, 129.7, 130.0, 136.6, 137.0, 149.7, 152.0, 159.0; FAB-MS (MNBA): m/z = 490 (100%, obsd), 490.23 (calcd for [M + H]$^+$).

Zn^{2+}–3 complex

The Zn^{2+}–**3** complex was prepared by mixing of equimolar quantities and gentle warming. All the volatile components were removed and the residue was characterised without further purification.

Complex Zn^{2+}–**3**: ^{1}H NMR (300 MHz, DMSO-d_6, 25 °C): δ 1.71 (br, 2H, $CH_2CH_2CH_2$), 2.67–2.83 (m + s, 10H, N(CH_3)$_2$ + CH_2CH_2NH + N$CH_2$$CH_2$), 4.02 (dd, J_1 16.3, J_2 16.3 Hz, 4H, PyCH_2N), 7.23 (d, J 7.5 Hz, 1H), 7.51–7.65 (m, 6H), 7.90 (br, 1H), 8.05–8.10 (m, 3H), 8.25 (d, J 8.6 Hz, 1H), 8.47 (d, J 8.5 Hz, 1H), 8.59 (d, J 4.9 Hz, 2H); FAB-MS (MNBA): m/z = 552 (100%, obsd), 552.14 (calcd for $C_{27}H_{30}N_5O_2SZn$).

Compounds 4 and 6

To a solution of 4-aminobutanol (103 μL, 1.12 mmol) in THF was added 0.9 equiv. of (Boc)$_2$O (218 mg, 1.00 mmol). After stirring for 1 h, the reaction mixture was set in an ice bath, then 156 μL of TEA (1.12 mmol) was added. To this reaction mixture was slowly added 1.1 equiv. of MsCl (100 μL) and the reaction mixture was stirred for 2 h. After the ice bath was removed, 10 mL of additional acetone and 10 equiv. of LiBr (972 mg) were added to the reaction mixture, which was then allowed to stir for 5 h. Subsequently all the volatile components were evaporated and the residue was partitioned between ethyl acetate and water. The organic phase was washed with water (×3), then dried in Na_2SO_4. Flash chromatographic purification (hexane–ethyl acetate = 1 : 2) afforded **c** (n = 4) (126 mg, 45% yield).

To a solution of **c** (n = 4) in acetonitrile were added 2 equiv. of KI (166 mg), 2 equiv. of K_2CO_3 (138 mg), and 2 equiv. of DPA (199 mg). After the reaction mixture had been moderately heated and refluxed for over 12 h, all the volatile components were evaporated and the residue was partitioned between ethyl acetate and water. The organic phase was washed with water (×3), then dried in Na_2SO_4. Flash chromatographic purification (MC–methanol = 20 : 1) followed by Boc deprotection with TFA, and coupling with 0.5 mmol of DsCl (134 mg) in the presence of 2.2 equiv. of TEA (153 μL) gave **4** (45 mg), which was acquired by extraction with ethyl acetate followed by gradient chromatographic purification (from hexane–ethyl acetate = 1 : 1 to MC–methanol = 20 : 1).

The same procedure was applied to the synthesis of **6**.

Compound **4**: ^{1}H NMR (300 MHz, $CDCl_3$, 25 °C): δ 1.27–1.46 (m, 4H, $CH_2CH_2CH_2CH_2$), 2.49 (t, 2H, J 6.2 Hz, N$CH_2$$CH_2$), 2.89 (s, 6H, N($CH_3$)$_2$), 2.93–3.01 (m, 2H, CH_2CH_2NH), 3.77 (s, 4H, PyCH_2N), 6.62 (br, 1H, NHSO$_2$), 7.14–7.18 (m, 3H), 7.36 (d, J 7.8 Hz, 2H), 8.24 (d, J 6.5 Hz, 1H), 8.40 (d, J 8.6 Hz, 1H), 8.52 (d, J 8.5 Hz, 1H), 8.57 (d, J 4.2 Hz, 2H); ^{13}C NMR (75 MHz, $CDCl_3$, 25 °C): δ 23.1, 27.8, 42.7, 45.8, 53.8, 53.8, 60.3, 115.4, 119.6, 122.7, 123.6, 124.1, 128.4, 129.6,

130.1, 130.3, 130.4, 136.2, 137.0, 149.5, 152.3; FAB-MS (MNBA): m/z = 504 (100%, obsd), 504.24 (calcd for $[M + H]^+$).

Compound **6**: ^{1}H NMR (300 MHz, $CDCl_3$, 25 °C): δ 1.08–1.43 (m, 6H, aliphatic CH_2), 2.47 (t, J 7.2 Hz, 2H, NCH_2CH_2), 2.81–2.88 (m, 8H, $N(CH_3)_2$ + CH_2CH_2NH), 3.80 (s, 4H, $PyCH_2N$), 4.98 (br, 1H, $NHSO_2$), 7.15–7.18 (m, 3H), 7.50–7.54 (m, 4H), 7.61–7.65 (m, 2H), 8.22–8.31 (d + d, J 8.6 Hz, 8.1 Hz, 2H), 8.51–8.54 (m, 3H); ^{13}C NMR (75 MHz, $CDCl_3$, 25 °C): δ 26.5, 26.8, 26.9, 29.9, 43.6, 45.8, 54.4, 60.7, 115.5, 119.1, 122.4, 123.4, 123.6, 128.7, 129.9, 130.0, 130.3, 130.7, 135.2, 136.9, 149.4, 152.4; FAB-MS (MNBA): m/z = 532 (71 %, obsd), 532.27 (calcd for $[M + H]^+$).

Acknowledgements

Financial support from CMDS (KOSEF) is gratefully acknowledged. T.W.K. and J.-h.P. thank the Ministry of Education for the award of BK 21 fellowships.

References

1 *Zinc and Health: Current Status and Future Directions*, *J. Nutr.*, 2000, **130**, Issue 5S.
2 For Zn^{2+} sensing in aqueous media: (*a*) T. Koike, T. Watanabe, S. Aoki, E. Kimura and M. Shiro, *J. Am. Chem. Soc.*, 1996, **118**, 12696–12703; (*b*) G. K. Walkup, S. C. Burdette, S. J. Lippard and R. Y. Tsien, *J. Am. Chem. Soc.*, 2000, **122**, 5644–5645; S. C. Burdette, G. K. Walkup, B. Spingler, R. Y. Tsien and S. J. Lippard, *J. Am. Chem. Soc.*, 2001, **123**, 7831–7841; (*c*) R. P. Cheng, S. L. Fisher and B. Imperiali, *J. Am. Chem. Soc.*, 1997, **119**, 3443–3450; (*d*) T. Hirano, K. Kikuch, Y. Urano, T. Higuchi and T. Nagano, *Angew. Chem., Int. Ed.*, 2000, **39**, 1052–1054; (*e*) C. J. Fahrni and T. V. O'Halloran, *J. Am. Chem. Soc.*, 1999, **121**, 11448–11458; (*f*) M. C. Kimber, I. B. Mahadevan, S. F. Lincoln, A. D. Ward and E. R. T. Tiekink, *J. Org. Chem.*, 2000, **65**, 8204–8209. For Zn^{2+} sensing in organic media; (*g*) J. D. Winkler, C. M. Bowen and V. Michelet, *J. Am. Chem. Soc.*, 1998, **120**, 3237–3242; (*h*) G. Hennrich, H. Sonnenschein and U. Resch-Genger, *J. Am. Chem. Soc.*, 1999, **121**, 5073–5074; (*i*) S. A. de Silva, A. Zavaleta and D. E. Baron, *Tetrahedron Lett.*, 1997, **38**, 2237–2240.
3 C. J. Frederickson, E. J. Kasarskis, D. Ringo and R. E. Frederickson, *J. Neurosci. Methods*, 1987, **20**, 91–103.
4 W.-J. Qian, C. A. Aspinwall, M. A. Battiste and R. T. Kennedy, *Anal. Chem.*, 2000, **72(4)**, 711–717.
5 http://www.probes.com/handbook/sections/2007.html.
6 T. Hirano, K. Kikuch, Y. Urano, T. Higuchi and T. Nagano, *J. Am. Chem. Soc.*, 2000, **122**, 12399–12400.
7 J. R. Lakowicz, *Principles of Fluorescence Spectroscopy*, Kluwer Academic/Plenum Publishers: New York, 1999, 2nd edition, Ch. 19.
8 R. M. Smith, A. E. Martell, *Critical Stability Constants*, Plenum Press: New York, 1975, vol. 2, p. 246.
9 (*a*) L. Prodi, M. Montalti, N. Zaccheroni, F. Dallavalle, G. Folesani, M. Lanfranchi, R. Corradini, S. Pagliari and R. Marchelli, *Helv. Chim. Acta*, 2001, **84**, 690–705; (*b*) A. Torrado, G. K. Walkup and B. Imperiali, *J. Am. Chem. Soc.*, 1998, **120**, 609–610.
10 (*a*) M. E. Huston, K. W. Haider and A. W. Czarnik, *J. Am. Chem. Soc.*, 1988, **110**, 4460–4462; (*b*) J. Yoon and A. W. Czarnik, *J. Am. Chem. Soc.*, 1992, **114**, 5874–5875.
11 K. A. Connors, *Binding Constants*, Wiley-Interscience, New York, 1987, pp. 24–28.
12 R. F. Chen and J. C. Kernohan, *J. Biol. Chem.*, 1967, **242**, 5813–5823.
13 J. Li and A. Eastman, *J. Biol. Chem.*, 1995, **270**, 3203–3211.